Delayed growth of Ewing sarcoma tumors associated with reduced expression and activity of Trk receptors, PI3K, and IGF1R

Bruna Almeida dos Santos [a,b,c], Natália Hogetop Freire [a,c,d], Livia Fratini [a], Matheus Dalmolin [c,e,f], Josimar Macedo de Castro [g], Marcelo A. C. Fernandes [c,e,f,h], Lauro Gregianin [a,c,i,j], André T. Brunetto [a,c,d], Algemir Lunardi Brunetto [a,c,d], Luis Fernando da Rosa Rivero [k], Mariane da Cunha Jaeger [a,c,d], Rafael Roesler [a,b,c,l], Caroline Brunetto de Farias [a,b,c,d]

[a]Cancer and Neurobiology Laboratory, Experimental Research Center, Clinical Hospital (CPE-HCPA), Federal University of Rio Grande do Sul, Porto Alegre, RS, Brazil; [b]Graduate Program in Biological Sciences: Pharmacology and Therapeutics, Institute for Basic Health Sciences, Federal University of Rio Grande do Sul, Porto Alegre, RS, Brazil; [c]National Science and Technology Institute for Children's Cancer Biology and Pediatric Oncology-INCT BioOncoPed, Porto Alegre, RS, Brazil; [d]Children's Cancer Institute (ICI), Porto Alegre, RS, Brazil; [e]InovAI Lab, nPITI/IMD, Federal University of Rio Grande do Norte, Natal, RN, Brazil; [f]Bioinformatics Multidisciplinary Environment (BioME), Federal University of Rio Grande do Norte, Natal, RN, Brazil; [g]Graduate Program in Medical Sciences, Faculty of Medicine, Federal University of Rio Grande do

Sul, Porto Alegre, RS, Brazil; [h]Department of Computer Engineering and Automation, Federal University of Rio Grande do Norte, Natal, RN, Brazil; [i]Department of Pediatrics, School of Medicine, Federal University of Rio Grande do Sul, Porto Alegre, RS, Brazil; [j]Pediatric Oncology Service, Clinical Hospital, Federal University of Rio Grande do Sul, Porto Alegre, RS, Brazil; [k]Department of Pathology, Faculty of Medicine, Federal University of Rio Grande do Sul, Porto Alegre, RS, Brazil; [l]Department of Pharmacology, Institute for Basic Health Sciences, Federal University of Rio Grande do Sul, Porto Alegre, RS, Brazil

CORRESPONDENCE: Caroline Brunetto de Farias. E-mail: cbfarias@zielbiosciences.com. Address: Cancer and Neurobiology Laboratory, Experimental Research Center, Clinical Hospital (CPE-HCPA), Federal University of Rio Grande do Sul. Rua Ramiro Barcelos, 2.350, 90035-003 Porto Alegre, RS, Brazil

ABSTRACT

Background: Ewing sarcoma (ES) is a childhood tumor that show features of mesenchymal and neural cell lineages. We have previously shown that tropomyosin receptor kinase (Trk) neurotrophin receptors regulate ES cell viability, and the pan-Trk and kinase inhibitor K252a restored sensitivity to chemotherapy in ES cells. Here, we show that systemic administration of K252a in mice delays ES tumor growth and reduces expression and activity of multiple targets.

Methods: BALB/c nu/nu nude mice inoculated with SK-ES-1 ES cells were given daily intraperitoneal (i.p.) injections of K252a for 18 days. Immunohistochemical analysis of tumors was performed to quantify the expression and phosphorylation of Trk receptors, phosphoinositide 3-kinase (PI3K), and insulin-like growth factor 1 receptor (IGF1R). The effect of combined therapy with K252a and an IGF1R inhibitor was tested in SK-ES-1 cells *in vitro*. Associations between expression of genes encoding Trks, PI3G, and IGF1R and overall survival (OS) in patients with ES was examined.

Results: Treatment with K252a led to a transient delay in ES tumor growth without affecting body weight or serum biochemical markers, and reduced the protein expression and phosphorylation of TrkA, TrkB, PI3K, and IGF1R. Combined treatment with K252a and the IGF1R inhibitor NVP-ADW742 was more effective in reducing ES cell viability than each compound alone. Significant associations between expression of *NTRK* genes and patient OS were found.

Conclusion: Inhibition of Trks, PI3K, and IGF1R can at least temporarily delay ES tumor growth. Moreover, *NTRK* genes should be further evaluated as biomarkers for prognosis in patients with ES.

KEYWORDS

Ewing sarcoma; K252a; Trk; *NTRK*; phosphoinositide 3-kinase; Insulin-like growth factor 1 receptor

Introduction

Ewing sarcoma (ES) is an aggressive type of childhood cancer that can arise either in bone or soft tissues, with a peak incidence during adolescence, though it also affects younger children and can occur at any age. ES tumors exhibit undifferentiated features that reflect elements of both mesenchymal and neural lineages. Although their exact cellular origin remains debated, current evidence suggests that ES may arise from neural crest–derived or mesenchymal stem cells, and that disruptions in epigenetic programming and multiple signaling pathways during embryonic development can contribute to tumor initiation and progression. At the genetic level, Ewing sarcoma is the prototypical example of a cancer driven by a specific chromosomal translocation. The translocations involve members of the FET (FUS, EWSR1, TAF15) and ETS transcription factor families, most commonly generating the EWS::FLI1 fusion oncogene. The resulting aberrant transcription factor reprograms gene expression and profoundly alters cell fate and differentiation potential, conferring the tumor's hallmark biological behavior. Therapeutically, the introduction of multimodal cytotoxic regimens has markedly improved outcomes for patients with localized disease, yielding survival rates of approximately 70–80%. However, prognosis remains poor for those with metastatic or relapsed ES, with long-term survival dropping to around 30%. Moreover, survivors frequently endure substantial, long-lasting adverse effects from treatment, including growth impairment, organ toxicity, and limb amputations, alongside the emotional and social challenges that come with surviving a severe childhood cancer. [1-6]

Given that the oncogenic fusion protein EWS::FLI1 by itself is hard to directly target with drugs, other components of the ES cell signaling landscape have been investigated as therapeutic targets. These include cell surface receptors such as receptor tyrosine kinases (RTKs). [7-10] Members of the RTK subfamily, tropomyosin receptor kinase (Trk) receptors include TrkA, TrkB, and TrkC, which are encoded by the *NTRK1*, *NTRK2*, and *NTRK3* genes, respectively. TrkA is the high-affinity receptor for nerve growth factor (NGF), while TrkB primarily binds brain-derived neurotrophic factor (BDNF) and neurotrophin-4 (NT-4). Neurotrophin-3 (NT-3) has the highest affinity for TrkC but can also to a lesser degree activate TrkA and TrkB. Upon ligand binding, Trk receptors undergo homodimerization and autophosphorylation at specific tyrosine residues, stimulating downstream cell signaling cascades that include the phosphoinositide 3-kinase (PI3K), mitogen-activated protein kinase (MAPK), and phospholipase C-γ (PLCγ)/protein kinase C (PKC) pathways. [11, 12] Beyond their physiological roles in the nervous system, Trk receptors have been increasingly implicated in tumor progression, therapy resistance, and cell survival in several types of cancer. [13-17] Trk inhibitors larotrectinib and entrectinib are currently used to treat patients with tumors harboring *NTRK* gene fusions, regardless of cancer type. [13, 18-21]

In a previous study, we reported that TrkA and TrkB are expressed in ES tumors, and treating ES cells to selective TrkA or TrkB inhibitors reduced cell proliferation, an effect that was increased when TrkA and TrkB were blocked simultaneously. [22] We then used the furanosylated indolocarbazole K252a, a microbial alkaloid originally isolated from the soil fungi *Nocardiopisis sp.* and structurally related to staurosporine, as a pan-Trk inhibitor. [23-26] Treatment with K252a induced changes in cell morphology, reduced β-III tubulin levels, and

decreased mRNA expression of NGF, BDNF, TrkA and TrkB. In addition, combining K252a with subeffective doses of cytotoxic chemotherapeutic drugs resulted in decreased ES cell proliferation and survival and restored sensitivity to chemotherapy in chemoresistant ES cells. [22] Here, we show that treatment with K252a delays ES tumor growth in mice and the effect is associated with inhibition of multiple tumor targets.

Materials and methods

Ethics statement

All experimental procedures with animals were conducted in accordance with the guidelines established by the National Council for Animal Control and Experimentation (CONCEA, Ministry of Science, Technology and Innovation, Brazil). All protocols used in this study were approved by the institutional Animal Care and Use Committee (CEUA, Hospital de Clínicas de Porto Alegre-HCPA), under project number 20190638).

Cell culture

SK-ES-1 ES cells were obtained from American Type Cell Collection (ATCC® HTB-86™) and verified for authenticity and lack of contamination. Cells were cultured and incubated in 5% CO_2 at 37°C in RPMI-1640 Medium (Gibco™, Thermo Fisher Scientific, Waltham, USA), supplemented with 1% amphotericin B, 5% 10,000 UI/mL penicillin 10 mg/ml streptomycin, and 10% fetal bovine serum (FBS, Gibco™, Thermo Fisher Scientific).

Drug treatment

K252a, methyl (13S,14R,16R)-14-hydroxy-13-methyl-5-oxo-6,7,13,14,15,16-hexahydro-5H-13,16-epoxydiindolo[1,2,3-fg:3′,2′,1′-kl]pyrrolo[3,4-i][1,6]benzodiazocine-14-carboxylate, (Sigma Aldrich, St. Louis, USA) and the selective Insulin-like growth factor 1 receptor (IGF1R) inhibitor NVP-ADW742 (Sigma Aldrich) were dissolved in dimethyl sulfoxide (DMSO, Sigma Aldrich). K252a was dissolved in saline solution (NaCl 0.9%) at the concentration of 2% DMSO in 98% saline for the treatment of mice at a dose of 0.5 mg/kg. Control mice were given vehicle (2% DMSO in 98% saline). For *in vitro* assays, cells were treated with the inhibitory concentration of 10% (IC10) of K252a (10 nM), NVP-ADW742 (196.6 nM) or K252a plus NVP-ADW742. Control cells were exposed to vehicle (DMSO 0.2%) in the culture medium.

Xenograft assay

Six-week-old nude mice (BALB/c nu/nu) from our own institutional breeding colony were used for the *in vivo* experiments. Mice were randomly distributed into two groups, K252a treatment and control. A cell line derived tumor xenograft (CDX) model was used to induce tumors. Animals were inoculated subcutaneously (s.c..) on the right dorsal flank with a suspension of SK-ES-1 cells (3×10^6). After the tumors reached 80 mm^3-100mm^3, the mice received intraperitoneal (i.p.) injections with K252a (0.5 mg/kg/day) or the same volume of vehicle (2% DMSO in 98% saline) once daily during 18 days. Body weight (g), tumor width (W) and tumor length (L) were measured every three days until

treatment day 18, and tumor volume (mm^3) was determined by the formula (W^2 x L)/2. At the end of the treatment, the mice were euthanized and the blood and tumors were collected for biochemical and histological analysis.

Biochemical markers

Heart blood was collected via puncture pre-euthanasia and serum was separated (at 3,000 rpm for 10 min) and stored at −80 °C. Alanine aminotransferase (ALT), aspartate aminotransferase (AST), creatinine and urea serum levels were evaluated by closed-circuit photometric assays (Cobas® c702, F. Hoffmann-La Roche Ltd., Basel, Switzerland).

Immunohistochemistry on tissue microarrays (TMA)

Tumors (n = 7 per group, removed immediately after the mouse's death) were fixed in 10% formalin to be included in paraffin blocks. Sections of three micrometers were used for the production of slides stained with hematoxylin-eosin (HE) as they served to evaluate the morphology and an area for the fabrication of the tissue microarray (TMA). A 2 mm block of TMA was used for the study, where duplicates were posted as the source area. Ten antibodies were used for tumor evaluation: TrkA polyclonal antibody (Product # PA5-90581), TrkB polyclonal antibody (Product # PA5-88293), phospho-TrkA (Tyr791) polyclonal antibody (Product # PA5-105456), TrkC polyclonal antibody pTyr516 (Product # PA5-39755), phospho-IGF1R polyclonal antibody (Tyr1165, Tyr1166) (Product # PA5-104772), PI3K p85 alpha polyclonal antibody (Product # PA5-29220), phospho-PI3 kinase p85 alpha pTyr607 polyclonal antibody (Product # PA5-

38905), phospho-TrkB polyclonal antibody pTyr515 (Product # PA5-38076), TrkC polyclonal antibody (Product # PA5-79766), TrkC polyclonal antibody (Product # PA5-79766), IGF1R (CD221) polyclonal antibody (Product # PA5-79445), and an anti-rabbit secondary antibody. The immunohistochemistry protocol (IHC) was carried out according to the specifications of each data sheet. The IHC assessment was scored semi-quantitatively according to intensity and distribution.

Cell viability

SK-ES-1 ES cells were seeded at a density of 4 X 10^3 cells per well in a complete medium into 96-well plates (Kasvi, Pinhais, Brazil). After 24 h, cells were treated with K252a, NVP-ADW742, or the two drugs combined, for 72 h and the medium was then removed, cells were washed with phosphate-buffered saline (PBS) and detached with 0.25% trypsin solution (Gibco™, Thermo Fisher Scientific). For cell viability analysis, the cell suspension was homogenized with trypan blue (BioSumos, Porto Alegre, Brazil) and counted in a hemocytometer. The mean of three independent experiments for each dose was used to calculate dose-response and combination index values.

Drug interactions

The combination index between the effects of K252a and NVP-ADW742 was calculated using the SinergyFinder/R version 4.1.3 package, [27] with cell viability of SK-ES-1 ES cells as input using the ZIP (Zero Interaction Potency) method.

Gene expression and survival analysis in ES patients

The gene expression dataset used for the survival analysis were obtained from the Gene Expression Omnibus (GEO) datasets accession numbers GSE63155 and GSE63156. The datasets GSE63155 and GSE63156 comprise expression data (Affymetrix Human Exon 1.0 ST Array) from primary ES tumor biopsies obtained from 46 patients from the Children's Oncology Group (COG) and 39 patients from the EuroEwing collaborative group respectively. [28] Microarray raw data (GSE63155 and GSE63156, Affymetrix Human Exon 1.0 ST Array, GPL5175) normalization (Robust Multichip Average, RMA method) and quality control were performed using the oligo *Bioconductor/R* version 4.3.1). Overall survival (OS) analysis for ES patients was done by Kaplan-Meier curves using the 'Survival' and 'Survminer' packages, to evaluate the effects of expression of each gene of interest namely the *NTRK1*, *NTRK2*, *NTRK3*, *IGF1R*, *PIK3CA* (which encodes the p110α protein, the catalytic subunit of the PI3K), and *PIK3R1* (which encodes a regulatory subunit of PI3K).

Statistical analysis

The Shapiro-Wilk test and histograms were used to verify the distribution of variables. An independent t-test was used for comparisons between groups, assuming a parametric distribution. Repeated measurements (body weight and tumor volume) were assessed by the Generalized Estimating Equation (GEE). The GEE model was modeled to identify statistical differences between treatment groups in mice (K252a versus controls), as well as tumor volume between

treatment days and the interaction between both factors. In the presence of a significant interaction indicated by $p < 0.05$, Bonferroni's correction was used for post-hoc multiple comparisons. The ordinal histology variables were analyzed using the Spearman's correlation method. All analyses were performed using the SPSS 20.0 software (IBM, Armonk, USA), assuming significance level at $p < 0.05$. Data are presented as mean and + standard error of the mean (S.E.M.).

Results

Systemic administration of K252a produces a transient delay in ES tumor growth

Treating nude mice inoculated with human SK-ES-1 ES cells with daily injections of K252a resulted in a significant reduction in tumor growth during treatment compared to controls. There were significant effects of treatment and time as well significant interactions between these factors (all *p*s < 0.01; **Figure 1B**, **1C**). The halt in tumor growth was apparent between treatment days 9 and 15. However, by day 18, tumor growth in the treatment group had recovered to levels comparable to those observed in the control group, suggesting that the drug effect was transient (**Figure 1B**). There were no significant differences between groups in body weight (**Figure 1D**) or serum biochemical markers, although apparent reductions in AST and ALT levels were observed in K252a-treated mice (**Figure 1E-H**).

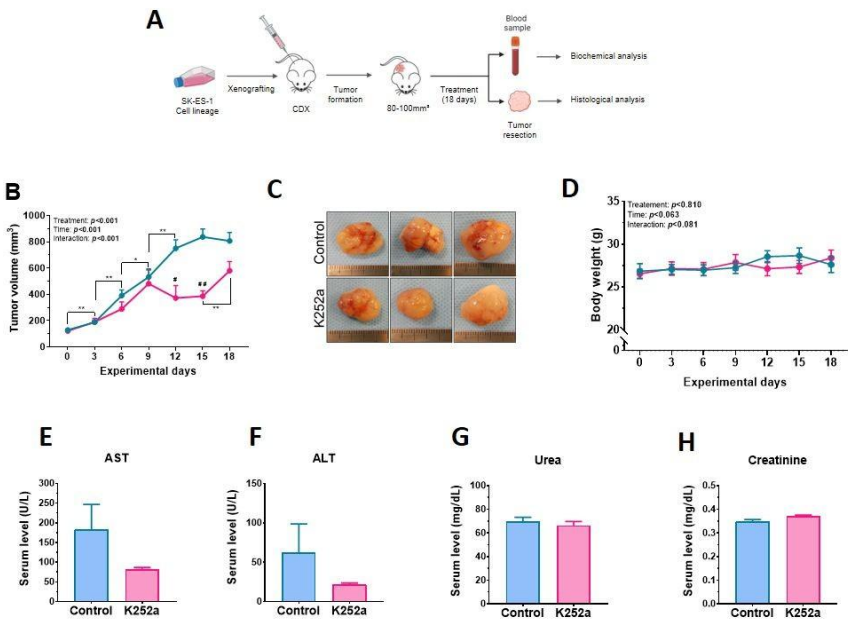

Figure 1. Treatment with K252a delays ES tumor growth. (**A**) Schematic of the experimental design. Human SK-ES-1 ES cells were xenografted into nude mice and the tumors were allowed to grow for 18 days. (**B**) tumor volume across experimental days. The blue line represents control mice and the pink line represents mice given K252a. The number of alive animals in each experimental day was: day 0, control, n = 14; K252a, n = 13; day 3, control, n = 14; K252a, n = 13; day 6, control, n = 14; K252a, n = 13; day 9, control, n = 14; K252a, n = 13; day 12, control, n = 14; K252a, n = 12; day 15, control, n = 11; K252a, n = 9; day 18, control, n = 7; K252a, n = 7; * $p < 0.05$, ** $p < 0.01$, comparisons between experimental days in each group. (**C**) Representative tumors from controls and K252-treated mice. (**D**) Body weight across experimental days; Serum levels of (**E**) AST, (F) ALT, (**G**) Urea, and (**H**) Creatinine in controls and K252a-treated mice (n = 7 per group).

Treatment with K252a reduces the protein expression and phosphorylation of TrkA, TrkB, PI3K, and IGF1R, without affecting TrkC in ES tumors

Tumors from mice treated with K252a had reduced protein levels of total (**Figure 2**) and phosphorylated (**Figure 3**) TrkA (total, $p = 0.06$, phosphorylated, $p = 0.04$),

TrkB (total, p = 0.05, phosphorylated, p = 0.012), and PI3K (total, p = 0.05, phosphorylated, p = 0.02), but unchanged TrkC levels. A subsequent analysis showed that K252a also reduced total and phosphorylated levels of IGF1R (total, p = 0.02, phosphorylated, p = 0.01; **Figure 4A**, **4B)**. Significant correlations were found in reduction of protein expression between several pairs of targets in cohorts of ES tumors from both groups of mice (**Supplementary Figure S1**).

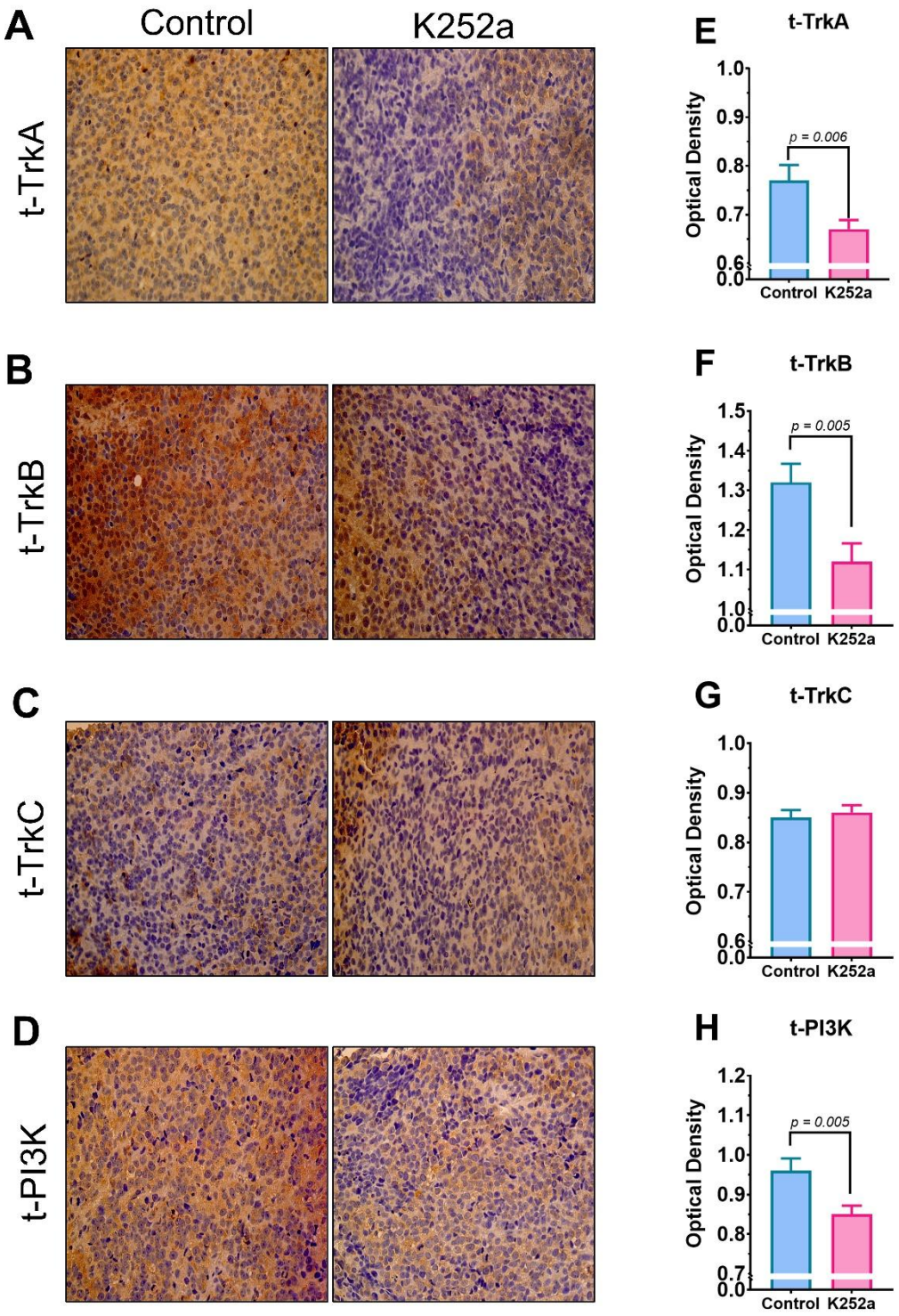

Figure 2. Immunohistochemical expression of total (phosphorylated and non-phosphorylated, t) (A, E) TrkA, (B, F) TrkB, (C, G) TrkC, and (D, H) PI3K in ES tumors from controls and K252a-treated mice (n = 7 per group). (A-D) Representative micrographs, X 40. (E-H) Protein content was quantified and shown as mean + S.E.M. optical density; *p* values are indicated in the panels.

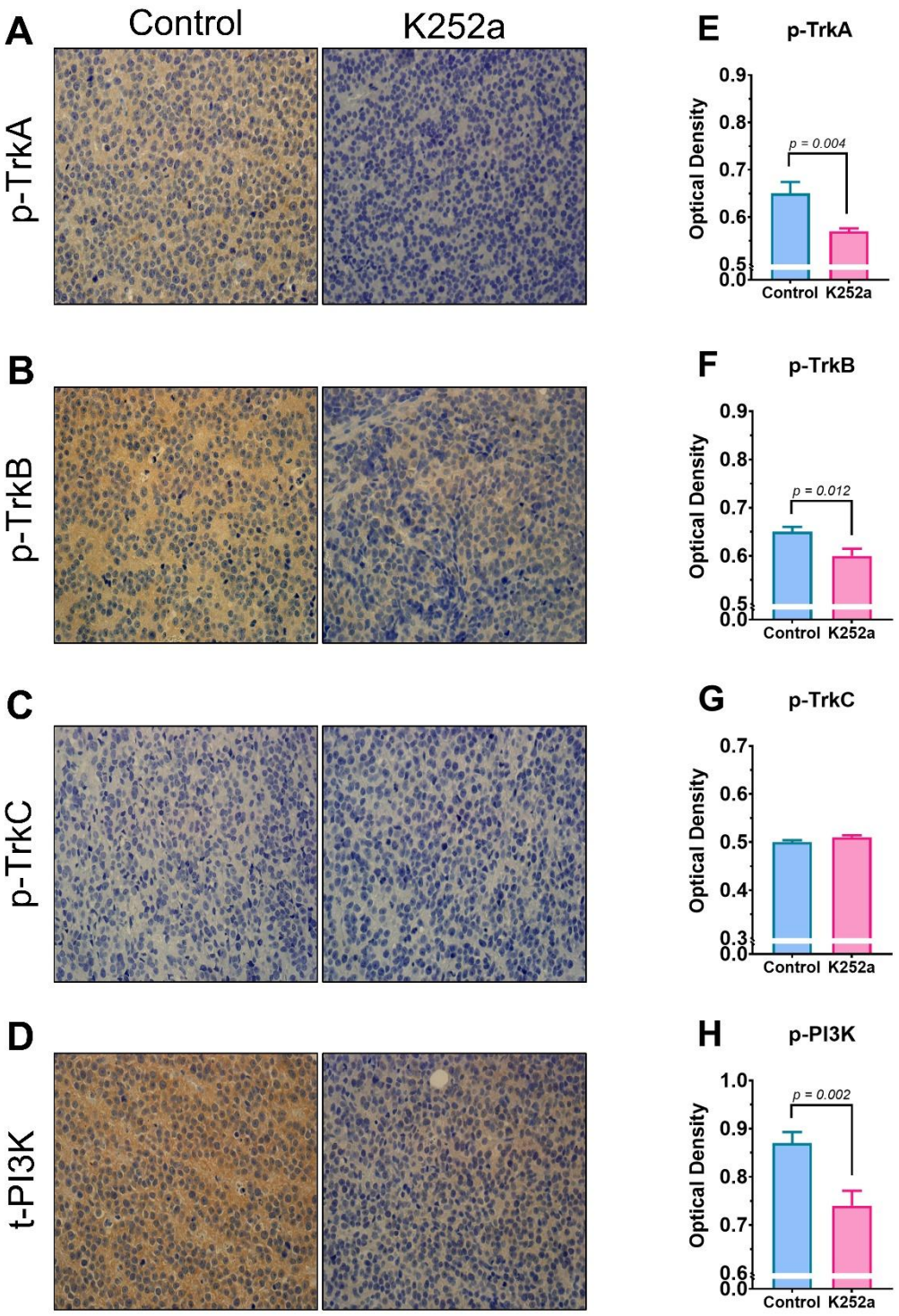

Figure 3. Immunohistochemical expression of phosphorylated (p) (A, E) TrkA, (B, F) TrkB, (C, G) TrkC, and (D, H) PI3K in ES tumors from controls and K252a-treated mice (n = 7 per group). (A-D) Representative micrographs, X 40. (E-H) Protein content was quantified and shown as mean + S.E.M. optical density; *p* values are indicated in the panels.

Combination treatment with K252a and an IGF1R inhibitor reduces ES cell viability

Exposure to K252a or NVP-ADW742 at doses equivalent to the IC10 resulted in a small but statistically significant reduction in the viability of SK-ES-1 ES cells. When the two drugs were used in combination, the resulting inhibition of cell viability was significantly more pronounced compared to the effects of each drug given alone (all *p*s < 0.05, **Figure 4C**). Significant synergism was demonstrated between the two drugs (25 and 75% quantiles = 19.29, **Figure 4D**).

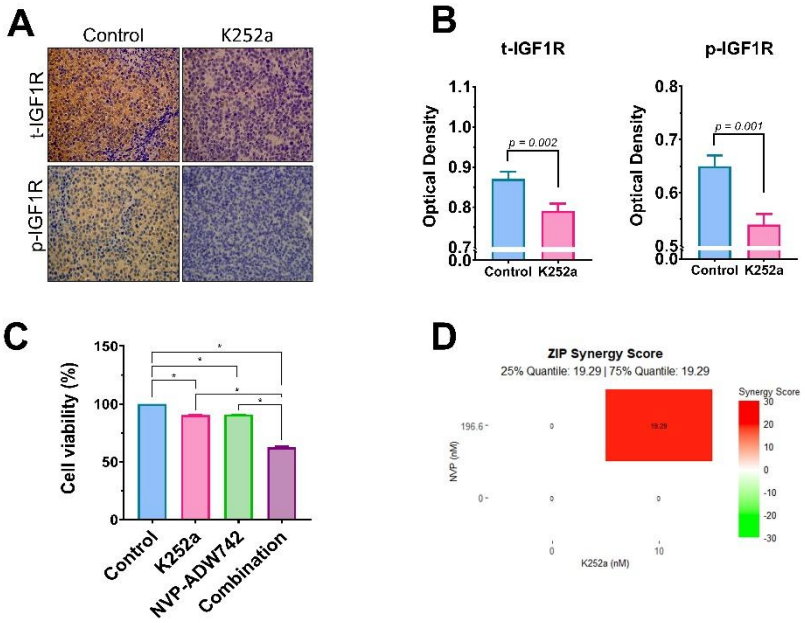

Figure 4. IGF1R expression and interaction with K252a in ES tumors. (A) Representative micrographs (X 40) of immunohistochemical expression for total(t-IGF1R) and phosphorylated (p-IGF1R) IGF1R in controls and K252a-treated mice (n = 7 per group). (B) Protein content was quantified and shown as mean + S.E.M. optical density; *p* values are indicated in the panels. (C) Viability of SK-ES-1 ES cells treated with K252a (10 nM), the IGF1R inhibitor NVP-ADW742 (196.6 nM), or the two inhibitors combined. Cell viability was assessed

by a trypan blue cell counting assay; n = 3 independent experiments, $p < 0.05$. (D) ZIP synergism score for the combination of K252a and NVP-ADW742.

***NTRK* gene expression is associated with OS in patients with ES**

TrkB, encoded by the *NTRK2* gene, is considered a preferred target of K252a inhibition. We found that higher *NTRK2* transcription is associated with worse prognosis assessed by shorter OS, specifically in the COG cohort ($p = 0.0042$, **Figure 5C**). In contrast, high *NTRK1* expression was associated with longer OS in the EuroEwing cohort ($p = 0.0049$, **Figure 5B**). *NTRK3* showed opposite patterns of association in the two datasets, indicating shorter OS in the COG cohort ($p = 0.0052$, **Figure 5E**) but longer OS in the EuroEwing cohort ($p = 0.013$, **Figure 5F**). No significant associations between gene expression and OS were found for *PIK3CA* (**Supplementary Figure S2A**, **S2B**), *PIK3R1* (**Supplementary Figure S2C**, **S2D**), or *IGF1R* (**Supplementary Figure S3**).

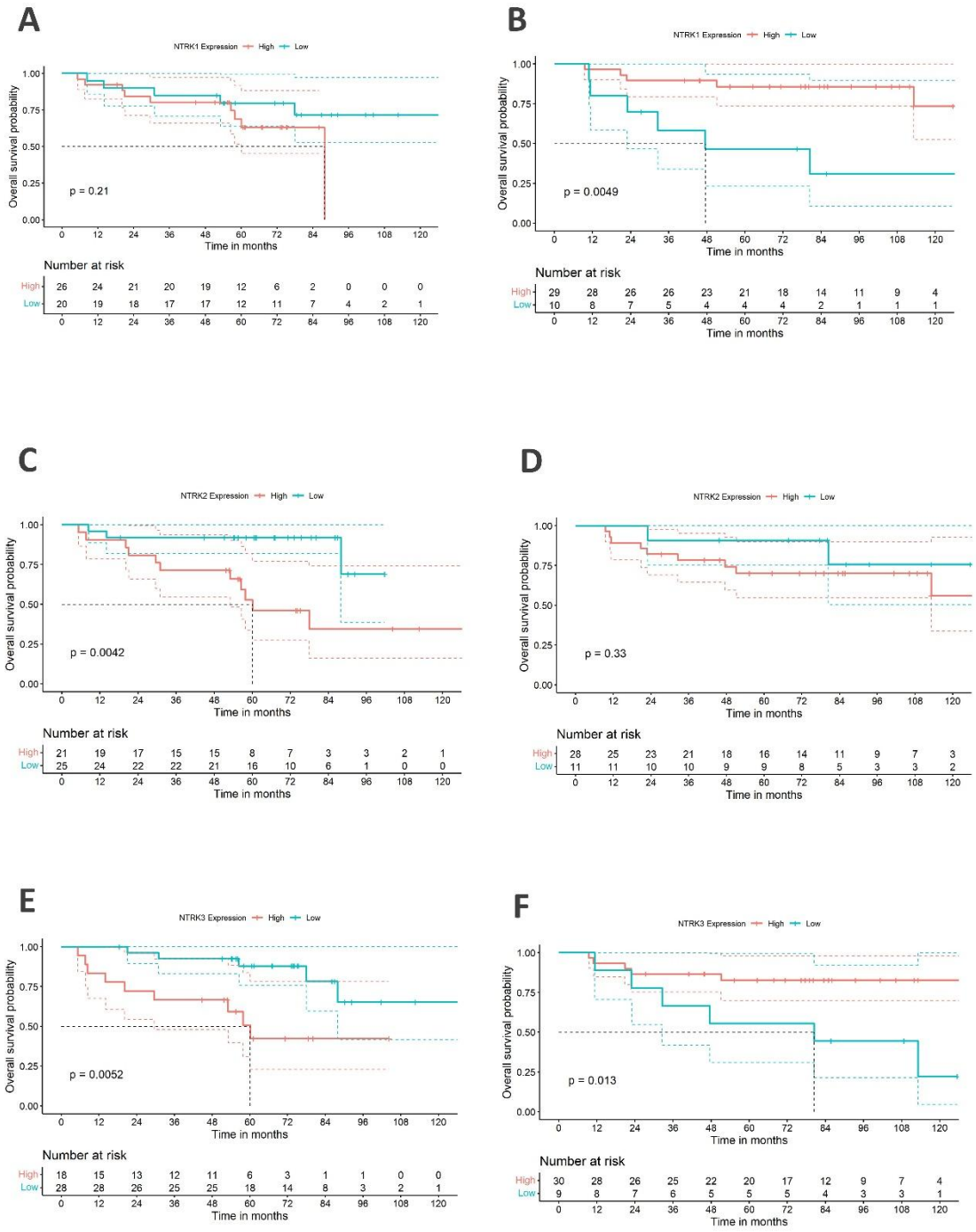

Figure 5. Associations between *NTRK* gene expression and prognosis assessed by OS in patients with ES. Datasets GSE63155 and GSE63156, comprising expression data from 46 primary ES tumors biopsies from COG and 39 tumors from the EuroEwing collaborative group respectively [28] were used (A) *NTRK1*, COG; (B) *NTRK1*, EuroEwing, (C) *NTRK2*, COG; (D) *NTRK2*, EuroEwing, (E) *NTRK3*, COG; (F) *NTRK3*, EuroEwing; *p* values are indicated in each panel.

Discussion

K252a has been widely used as a tool to investigate Trk-mediated signaling, particularly for TrkB, due to its potent inhibitory effects on Trks at nanomolar concentrations. However, at higher or even similar concentrations, and certainly at the doses we used in our *in vivo* experiment, it can also directly inhibit several other protein kinases. [29-33] Therefore, it is more accurate to interpret our findings as reflecting the effects of a non-specific, multi-kinase inhibitor, rather than those of a TrkB or pan-Trk inhibitor. Administration of K252a was able to significantly reduce the protein content and phosphorylation (a biochemical surrogate for kinase activation) of TrkA, TrkB, PI3K, and IGF1R in SK-ES-1 ES tumor xenografts, raising the possibility that either direct or indirect inhibition of these targets at least partially mediates the effect of K252a on tumor growth. Our correlation analysis showed that the expression of p-PI3K was positively associated with the content of both p-TrkA and p-TrkB, supporting the possibility that PI3K is among the downstream targets of Trk inhibition.

Consistent with the possibility, raised by our previous study, [22] that TrkA and TrkB expression and signaling influence ES growth, we found that higher *NTRK2* gene expression can be associated with worse prognosis assessed by OS, whereas high *NTRK1* expression indicates longer OS. These effects were observed specifically in one of the two cohorts examined, so that significant effects were found for *NTRK1* in the EuroEwing dataset and for *NTRK2* in the COG dataset. Contrasting patterns between the two patient cohorts were found for *NTRK3*; high gene expression was associated with a shorter OS in the COG

dataset but longer OS in the EuroEwing dataset. We previously found a similar association between high *NTRK3* transcription and longer survival in patients with medulloblastoma, the main type of pediatric brain tumor. [17] Both *NTRK1* and *NTRK3* can act either as oncogenes or tumor suppressor genes. *NTRK1* is a tumor suppressor inhibited by methylation in ovarian cancer and endometrial hyperplasia. [34, 35] Reconstitution of normal *NTRK3* expression previously suppressed by aberrant hypermethylation induces apoptosis in colon tumors, [36] and *NTRK3* is a tumor suppressor gene inactivated by methylation also in cervical cancer. [37] However, the first study reporting a role for the *NTRK3* product, TrkC, in ES found the receptor to be frequently overexpressed in human metastatic ES cells, promoting cell survival, tumorigenicity, and metastasis, and loss of TrkC expression reduced experimental ES tumor growth and metastasis in mice. [38]

Overexpression of IGF1R has been associated with more aggressive tumors and worse outcomes in ES, although our own transcriptional analysis did not reveal an association between IGF1R mRNA expression and survival of ES patients. Monoclonal antibodies targeting IGF1R have been developed and tested clinically in patients with ES in several trials, although the clinical efficacy remains to be fully established. [39-44] Another novel finding reported in the present study is that the combination of K252a with an IGF1R inhibitor was more efficient in reducing ES cell viability than each drug given alone, highlighting the importance of evaluating combinatorial therapeutic regimens involving IGF1R inhibitors and drugs targeting Trks and protein kinases. [45]

We describe the successful growth of ES tumors using SK-ES-1 cells xenografted into nude mice. Previous studies have used other cell types to induce

ES tumors in mice, [46-47] thus one contribution of our study is to establish a SK-ES-1 mouse model of ES. However, this study has several limitations. Patient-derived xenograft (PDX) mouse models, defined as models developed from direct implantation of patient tumor tissue into immunodeficient mice without prior cell culture or expansion, are now considered the gold standard for *in vivo* preclinical drug testing, and a number of such models have been developed for ES and other pediatric solid tumors. [48] It is also worth noting that our experiments do not allow to determine whether the reductions in target expression and phosphorylation are due to direct inhibition by K252a or downstream to drug-induced inhibition of Trks or other kinases. Future experiments should explore in detail the effects of selective TrkA, TrkB, and PI3K inhibitors, and compare them with multi-kinase inhibitors.

Conclusion

In summary, we report evidence suggesting that the combined inhibition of Trks, PI3K, and IGF1R by a multi-kinase inhibitor can delay ES tumor growth (summarized in **Figure 6**). In addition, *NTRK* genes should be further evaluated as potential biomarkers for prognosis in patients with ES.

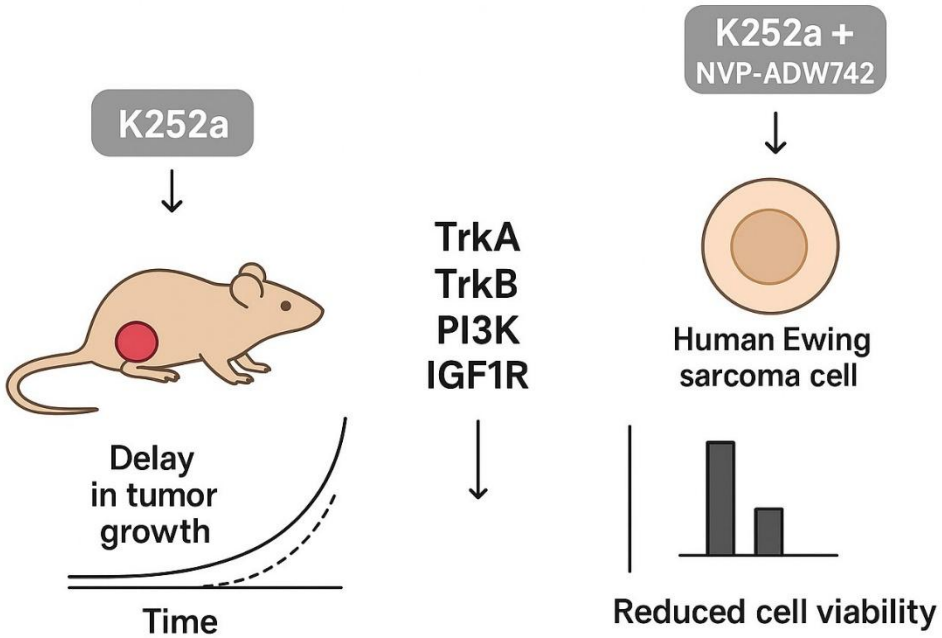

Figure 6. Schematic model highlighting selected aspects of K252a effects on ES. Systemic administration of K252a delays the growth of human SK-ES-1 ES tumors xenografted into nude mice and the effect is associated with reduced expression and phosphorylation of TrkA, TrkB, PI3K, and IGF1R in the tumors. Combined exposure to K252a and the IGF1R inhibitor NVP-ADW742 reduces SK-ES-1 ES cell viability more effectively than each compound alone.

Disclosure statement

No potential conflict of interest was reported by the authors.

Funding

This research was supported by PRONON/Ministry of Health, Brazil (number 25000.202751/2016-65); National Council for Scientific and Technological

Development (CNPq) grant numbers 304623/2025-3 and 406484/2022-8-INCT BioOncoPed to R.R.; the Children's Cancer Institute (ICI); the Coordination for the Improvement of Higher Education Personnel (CAPES); and the Clinical Hospital institutional research fund (FIPE-HCPA number 20190638).

Data availability statement

The ES tumor datasets GSE63155 and GSE63156, [28] used for the analyses of associations between gene expression and patient survival presented in this study, are available at https://www.ncbi.nlm.nih.gov/geo/query/acc.cgi?acc=GSE63155 and https://www.ncbi.nlm.nih.gov/geo/query/acc.cgi?acc=GSE63156, respectively. Other data presented in this study may be obtained from the corresponding author upon request.

Author contributions

B.A.S. and C.B.F. conceived and designed the experiments. B.A.S., N.H.F., L.F., M.D., J.M.C., L.F.R.R., and M.C.J. conducted the experimental study and data analyses; B.A.S., R.R., and C.B.F. wrote the manuscript. M.A.C.F., L.G., A.T.B., A.L.B., M.C.J., R.R., and C.B.F. provided support and supervised the research. All authors revised and approved the submitted manuscript.

References

1. dos Santos RP, Roesler R, Gregianin L, Brunetto AT, da Cunha Jaeger M, Lunardi Brunetto A, de Farias CB. Cancer stem cells and chemoresistance in Ewing sarcoma. Curr Stem Cell Res Ther. 2023;18(7): 926-936. doi: 10.2174/1574888X17666220627114710.

2. Dupuy M, Lamoureux F, Mullard M, Postec A, Regnier L, Baud'huin M, Georges S, Brounais-Le Royer B, Ory B, Rédini F, Verrecchia F. Ewing sarcoma from molecular biology to the clinic. Front Cell Dev Biol. 2023;11: 1248753. doi: 10.3389/fcell.2023.1248753.

3. Gregianin LJ, Rose A, Villarroel M, Almeida MT, Siqueira L, Salgado C, da Costa GA, Castillo L, Santos Pestilho JFC, Brunetto AL; GALOP Latin American Pediatric Oncology Group Ewing Sarcoma Investigators. Results of the Latin American Pediatric Oncology Group (GALOP-2011) trial for patients with localized Ewing sarcoma: A multicentric study of interval-compressed multiagent chemotherapy. Pediatr Blood Cancer. 2025;72(4): e31554. doi: 10.1002/pbc.31554.

4. Gupta A, Dietz MS, Riedel RF, Dhir A, Borinstein SC, Isakoff MS, Aye JM, Rainusso N, Armstrong AE, DuBois SG, Wagner LM, Rosenblum JM, Cohen-Gogo S, Albert CM, Zahler S, Chugh R, Trucco M. Consensus recommendations for systemic therapies in the management of relapsed Ewing sarcoma: A report from the National Ewing Sarcoma Tumor Board. Cancer. 2024;130(23): 4028-4039. doi: 10.1002/cncr.35537.

5. Riggi N, Suvà ML, Stamenkovic I. Ewing's Sarcoma. N Engl J Med. 2021;384(2): 154-164. doi: 10.1056/NEJMra2028910.

6. Zöllner SK, Amatruda JF, Bauer S, Collaud S, de Álava E, DuBois SG, Hardes J, Hartmann W, Kovar H, Metzler M, Shulman DS, Streitbürger A, Timmermann B, Toretsky JA, Uhlenbruch Y, Vieth V, Grünewald TGP, Dirksen U. Ewing sarcoma-diagnosis, treatment, clinical challenges and future perspectives. J Clin Med. 2021;10(8): 1685. doi: 10.3390/jcm10081685.

7. Daley JD, Whiteway SL, Heske CM, Dela Cruz FS, Whittle SB, Cohen-Gogo S, Collier AB, Gupta A, Ohm J, Clark A, Soragni A, Lawlor E, Setty B, Grohar PJ, Janeway K, Reed DR, Slotkin EK, Bailey KM. New approaches to investigate novel agents in Ewing sarcoma: A report from the Children's Oncology Group Bone Tumor Committee. Pediatr Blood Cancer. 2025;72(10): e31917. doi: 10.1002/pbc.31917.

8. Fayzullina D, Tsibulnikov S, Stempen M, Schroeder BA, Kumar N, Kharwar RK, Acharya A, Timashev P, Ulasov I. Novel targeted therapeutic strategies for Ewing sarcoma. Cancers (Basel).2022;14(8): 1988. doi: 10.3390/cancers14081988.

9. Jia K, Cao L, Yu Y, Jing D, Wu W, Van Tine BA, Shao Z. Signaling pathways and targeted therapies in Ewing sarcoma. Pharmacol Ther. 2025;266: 108765. doi: 10.1016/j.pharmthera.2024.108765.

10. Just MA, Van Mater D, Wagner LM. Receptor tyrosine kinase inhibitors for the treatment of osteosarcoma and Ewing sarcoma. Pediatr Blood Cancer. 2021;68(8): e29084. doi: 10.1002/pbc.29084.

11. Bothwell M. Recent advances in understanding neurotrophin signaling. F1000Res. 2016;5: F1000 Faculty Rev-1885. doi: 10.12688/f1000research.8434.1.

12. Park H, Poo MM. Neurotrophin regulation of neural circuit development and function. Nat Rev Neurosci. 2013;14(1): 7-23. doi: 10.1038/nrn3379.

13. Amatu A, Sartore-Bianchi A, Bencardino K, Pizzutilo EG, Tosi F, Siena S. Tropomyosin receptor kinase (TRK) biology and the role of NTRK gene fusions in cancer. Ann Oncol. 2019;30(Suppl_8): viii5-viii15. doi: 10.1093/annonc/mdz383.

14. Meldolesi J. Neurotrophin Trk receptors: New targets for cancer therapy. Rev Physiol Biochem Pharmacol. 2018;174: 67-79. doi: 10.1007/112_2017_6.

15. Roesler R, de Farias CB, Abujamra AL, Brunetto AL, Schwartsmann G. BDNF/TrkB signaling as an anti-tumor target. Expert Rev Anticancer Ther. 2011;11(10): 1473-1475. doi: 10.1586/era.11.150

16. Thiele CJ, Li Z, McKee AE. On Trk--the TrkB signal transduction pathway is an increasingly important target in cancer biology. Clin Cancer Res. 2009;15(19): 5962-5967. doi: 10.1158/1078-0432.CCR-08-0651.

17. Thomaz A, Jaeger M, Brunetto AL, Brunetto AT, Gregianin L, de Farias CB, Ramaswamy V, Nör C, Taylor MD, Roesler R. Neurotrophin signaling in medulloblastoma. Cancers (Basel). 2020;12(9): 2542. doi: 10.3390/cancers12092542.

18. Amatu A, Sartore-Bianchi A, Siena S. NTRK gene fusions as novel targets of cancer therapy across multiple tumour types. ESMO Open. 2016;1(2): e000023. doi: 10.1136/esmoopen-2015-000023.

19. Drilon A, Laetsch TW, Kummar S, DuBois SG, Lassen UN, Demetri GD, Nathenson M, Doebele RC, Farago AF, Pappo AS, Turpin B, Dowlati A, Brose MS, Mascarenhas L, Federman N, Berlin J, El-Deiry WS, Baik C, Deeken J, Boni V, Nagasubramanian R, Taylor M, Rudzinski ER, Meric-Bernstam F, Sohal DPS, Ma PC, Raez LE, Hechtman JF, Benayed R, Ladanyi M, Tuch BB, Ebata K, Cruickshank S, Ku NC, Cox MC, Hawkins DS, Hong DS, Hyman DM. Efficacy of larotrectinib in TRK fusion-positive cancers in adults and children. N Engl J Med. 2018;378(8): 731-739. doi: 10.1056/NEJMoa1714448.

20. Laetsch TW, Hong DS. Tropomyosin receptor kinase inhibitors for the treatment of TRK fusion cancer. Clin Cancer Res. 2021;27(18): 4974-4982. doi: 10.1158/1078-0432.CCR-21-0465.

21. Nasehi P, Omidkhah N, Ghodsi R. A review: Recent developments of co-targeted TRK (tropomyosin receptor kinases) inhibitors for cancer therapy. Bioorg Chem. 2025;165: 108950. doi: 10.1016/j.bioorg.2025.108950.

22. Heinen TE, Dos Santos RP, da Rocha A, Dos Santos MP, Lopez PL, Silva Filho MA, Souza BK, Rivero LF, Becker RG, Gregianin LJ, Brunetto AL, Brunetto AT, de Farias CB, Roesler R. Trk inhibition reduces cell proliferation and potentiates the effects of chemotherapeutic agents in Ewing sarcoma. Oncotarget. 2016;7(23): 34860-34880. doi: 10.18632/oncotarget.8992.

23. Chiu HT, Chen YL, Chen CY, Jin C, Lee MN, Lin YC. Molecular cloning, sequence analysis and functional characterization of the gene cluster for biosynthesis of K-252a and its analogs. Mol Biosyst. 2009;5(10): 1180-1191. doi: 10.1039/b905293c.

24. Kase H, Iwahashi K, Matsuda Y. K-252a, a potent inhibitor of protein kinase C from microbial origin. J Antibiot (Tokyo). 1986;39(8): 1059-1065. doi: 10.7164/antibiotics.39.1059.

25. Lazarovici P, Rasouly D, Friedman L, Tabekman R, Ovadia H, Matsuda Y. K252a and staurosporine microbial alkaloid toxins as prototype of neurotropic drugs. Adv Exp Med Biol. 1996;391: 367-377. doi: 10.1007/978-1-4613-0361-9_31.

26. Nakanishi S, Yamada K, Kase H, Nakamura S, Nonomura Y. K-252a, a novel microbial product, inhibits smooth muscle myosin light chain kinase. J Biol Chem. 1988;263(13): 6215-6219.

27. Zheng S, Wang W, Aldahdooh J, Malyutina A, Shadbahr T, Tanoli Z, Pessia A, Tang J. SynergyFinder Plus: Toward better interpretation and annotation

of drug combination screening datasets. Genomics Proteomics Bioinformatics. 2022;20(3): 587-596. doi: 10.1016/j.gpb.2022.01.004.

28. Volchenboum SL, Andrade J, Huang L, Barkauskas DA, Krailo M, Womer RB, Ranft A, Potratz J, Dirksen U, Triche TJ, Lawlor ER. Gene expression profiling of Ewing sarcoma tumors reveals the prognostic importance of tumor-stromal interactions: A report from the Children's Oncology Group. J Pathol Clin Res. 2015;1(2): 83-94. doi: 10.1002/cjp2.9.

29. Gschwendt M, Leibersperger H, Marks F. Differentiative action of K252a on protein kinase C and a calcium-unresponsive, phorbol ester/phospholipid-activated protein kinase. Biochem Biophys Res Commun. 1989;164(3): 974-982. doi: 10.1016/0006-291x(89)91765-8.

30. Hashimoto Y, Nakayama T, Teramoto T, Kato H, Watanabe T, Kinoshita M, Tsukamoto K, Tokunaga K, Kurokawa K, Nakanishi S, et al. Potent and preferential inhibition of Ca2+/calmodulin-dependent protein kinase II by K252a and its derivative, KT5926. Biochem Biophys Res Commun. 1991;181(1): 423-429. doi: 10.1016/s0006-291x(05)81436-6.

31. Mizuno K, Saido TC, Ohno S, Tamaoki T, Suzuki K. Staurosporine-related compounds, K252a and UCN-01, inhibit both cPKC and nPKC. FEBS Lett. 1993;330(2): 114-116. doi: 10.1016/0014-5793(93)80254-r.

32. Pan J, Wang G, Yang HQ, Hong Z, Xiao Q, Ren RJ, Zhou HY, Bai L, Chen SD. K252a prevents nigral dopaminergic cell death induced by 6-hydroxydopamine through inhibition of both mixed-lineage kinase 3/c-Jun NH2-terminal kinase 3 (JNK3) and apoptosis-inducing kinase 1/JNK3 signaling pathways. Mol Pharmacol. 2007;72(6): 1607-1618. doi: 10.1124/mol.107.038463.

33. Tapley P, Lamballe F, Barbacid M. K252a is a selective inhibitor of the tyrosine protein kinase activity of the trk family of oncogenes and neurotrophin receptors. Oncogene. 1992;7(2): 371-381.

34. Chmelařová M, Dvořáková E, Špaček J, Laco J, Mžik M, Palička V. Promoter methylation of GATA4, WIF1, NTRK1 and other selected tumour suppressor genes in ovarian cancer. Folia Biol (Praha). 2013;59(2): 87-92.

35. Dvořák O, Slavíčková M, Laco J, Štěpán M, Čermáková E, Špaček J. DNA hypermethylation of tumor suppressor genes TWIST1, GATA4, MUS81 and NTRK1 in endometrial hyperplasia. Ceska Gynekol. 2024;89(4): 261-268. doi: 10.48095/cccg2024261.

36. Luo Y, Kaz AM, Kanngurn S, Welsch P, Morris SM, Wang J, Lutterbaugh JD, Markowitz SD, Grady WM. NTRK3 is a potential tumor suppressor gene commonly inactivated by epigenetic mechanisms in colorectal cancer. PLoS Genet. 2013;9(7): e1003552. doi: 10.1371/journal.pgen.1003552.

37. Ji H, Li K, Jiang W, Li J, Zhang JA, Zhu X. MRVI1 and NTRK3 are potential tumor suppressor genes commonly inactivated by DNA methylation in cervical cancer. Front Oncol. 2022;11: 802068. doi: 10.3389/fonc.2021.802068.

38. Kim MS, Lee WS, Lee H, Jin W. TrkC, a novel prognostic marker, induces and maintains cell survival and metastatic dissemination of Ewing sarcoma by inhibiting EWSR1-FLI1 degradation. Cell Death Dis. 2022;13(9): 836. doi: 10.1038/s41419-022-05275-w.

39. Anderson PM, Bielack SS, Gorlick RG, Skubitz K, Daw NC, Herzog CE, Monge OR, Lassaletta A, Boldrini E, Pápai Z, Rubino J, Pathiraja K, Hille DA, Ayers M, Yao SL, Nebozhyn M, Lu B, Mauro D. A phase II study of clinical activity of SCH 717454 (robatumumab) in patients with relapsed osteosarcoma and Ewing sarcoma. Pediatr Blood Cancer. 2016;63(10): 1761-1770. doi: 10.1002/pbc.26087.

40. Juergens H, Daw NC, Geoerger B, Ferrari S, Villarroel M, Aerts I, Whelan J, Dirksen U, Hixon ML, Yin D, Wang T, Green S, Paccagnella L, Gualberto A. Preliminary efficacy of the anti-insulin-like growth factor type 1 receptor antibody figitumumab in patients with refractory Ewing sarcoma. J Clin Oncol. 2011;29(34): 4534-4540. doi: 10.1200/JCO.2010.33.0670.

41. Naing A, LoRusso P, Fu S, Hong DS, Anderson P, Benjamin RS, Ludwig J, Chen HX, Doyle LA, Kurzrock R. Insulin growth factor-receptor (IGF-1R) antibody cixutumumab combined with the mTOR inhibitor temsirolimus in patients with refractory Ewing's sarcoma family tumors. Clin Cancer Res. 2012;18(9): 2625-2631. doi: 10.1158/1078-0432.CCR-12-0061.

42. Olmos D, Postel-Vinay S, Molife LR, Okuno SH, Schuetze SM, Paccagnella ML, Batzel GN, Yin D, Pritchard-Jones K, Judson I, Worden FP, Gualberto A, Scurr M, de Bono JS, Haluska P. Safety, pharmacokinetics, and preliminary activity of the anti-IGF-1R antibody figitumumab (CP-751,871) in patients with sarcoma and Ewing's sarcoma: a phase 1 expansion cohort study. Lancet Oncol. 2010;11(2): 129-135. doi: 10.1016/S1470-2045(09)70354-7.

43. Pappo AS, Patel SR, Crowley J, Reinke DK, Kuenkele KP, Chawla SP, Toner GC, Maki RG, Meyers PA, Chugh R, Ganjoo KN, Schuetze SM, Juergens H, Leahy MG, Geoerger B, Benjamin RS, Helman LJ, Baker LH.

R1507, a monoclonal antibody to the insulin-like growth factor 1 receptor, in patients with recurrent or refractory Ewing sarcoma family of tumors: results of a phase II Sarcoma Alliance for Research through Collaboration study. J Clin Oncol. 2011;29(34): 4541-4547. doi: 10.1200/JCO.2010.34.0000.

44. Tap WD, Demetri G, Barnette P, Desai J, Kavan P, Tozer R, Benedetto PW, Friberg G, Deng H, McCaffery I, Leitch I, Badola S, Chang S, Zhu M, Tolcher A. Phase II study of ganitumab, a fully human anti-type-1 insulin-like growth factor receptor antibody, in patients with metastatic Ewing family tumors or desmoplastic small round cell tumors. J Clin Oncol. 2012;30(15): 1849-1856. doi: 10.1200/JCO.2011.37.2359.

45. Assi A, Farhat M, Mohanna R, Hachem MCR, Zalaquett Z, Aoun M, Farraj SA, Daher M, Sebaaly A, Kourie HR. Tyrosine kinase inhibitors in Ewing's sarcoma: a systematic review. BMC Cancer. 2025;25(1): 735. doi: 10.1186/s12885-025-14130-y.

46. Vormoor J, Baersch G, Decker S, Hotfilder M, Schäfer KL, Pelken L, et al. Establishment of an in vivo model for pediatric Ewing tumors by transplantation into NOD/scid mice. Pediatr Res. 2001;49: 332-341. doi: 10.1203/00006450-200103000-00006.

47. Vormoor B, Knizia HK, Batey MA, Almeida GS, Wilson I, Dildey P, et al. Development of a preclinical orthotopic xenograft model of Ewing sarcoma and other human malignant bone disease using advanced in vivo imaging. PLoS One. 2014;9: e85128. doi: 10.1371/journal.pone.0085128.

48. Dela Cruz FS, Stewart EA, Surdez D, Daley JD, Soragni A, Tomazou EM, Alvarez-Perez J, Feinberg TY, Amatruda JF, Ganapathi SS, Ohm JE, Heske CM, Cohen-Gogo S, Pesic D, Nash JO, Shlien A, Roundhill EA, Burchill SA, Crompton BD, Lawlor ER, Loeb DM, Delattre O, Mora J, Scotlandi K, Reed DR, Grohar PJ, Grünewald TGP, Kovar H, Bailey KM. Advancing preclinical biology for Ewing sarcoma: An international effort. Mol Cancer Ther. 2025:OF1-OF23. doi: 10.1158/1535-7163.MCT-25-0428.